



1 The flexural strength of bonded ice

2 Andrii Murdza¹, Arttu Polojärvi², Erland M. Schulson¹, Carl E. Renshaw^{1,3}

3 ¹Thayer School of Engineering, Dartmouth College, Hanover, NH, USA

4 ²Aalto University, School of Engineering, Department of Mechanical Engineering, P.O. Box 14100, 00076 Aalto,
5 Finland

6 ³Department of Earth Sciences, Dartmouth College, Hanover, NH, USA

7 *Correspondence to:* Andrii Murdza (Andrii.Murdza@dartmouth.edu)

8 **Abstract.** The flexural strength of ice surfaces bonded by freezing, termed freeze-bond, was studied by performing
9 four-point-bending tests of bonded freshwater S2 columnar-grained ice samples in the laboratory. The samples were
10 prepared by milling the surfaces of two ice pieces, wetting two of the surfaces with water of varying salinity, bringing
11 these surfaces together, and then letting them freeze under a compressive stress of about 4 kPa. The salinity of the
12 water used for wetting the surfaces to generate the bond varied from 0 to 35 ppt. Freezing occurred in air under
13 temperatures varying from -25 to -3 °C over periods that varied from 0.5 h to ~100 hours. Results show that an increase
14 in bond salinity or temperature leads to a decrease in bond strength. The trend for the bond strength as a function of
15 salinity is similar to that presented in Timco and O'Brien (1994) for saline ice. No freezing occurs at -3 °C once the
16 salinity of the water used to generate the bond exceeds ~25 ppt. The strength of the saline ice bonds levels off (i.e.,
17 saturates) within 6-12 hours of freezing; bonds formed from fresh water reach strengths that are comparable or higher
18 than that of the parent material in less than 0.5 hours.

19 1. Introduction

20 Freeze bonds form when distinct ice features, such as floating ice floes or ice blocks of a rubble pile, become
21 and remain in contact over a period of time at low enough temperature. Insight into the strength of the bonds is
22 important when, for example, the strength of an ice cover formed of refrozen floes or the strength of an ice rubble pile
23 is estimated. There are several factors that affect the failure of a cover of sea ice, surface waves being a major one
24 that has gained an increasing amount of interest recently (Shen, 2017; Squire, 2020). Under the action of waves, ice
25 covers bend and may undergo flexural failure (Ardhuin et al., 2020; Asplin et al., 2012; Collins et al., 2015; Hwang
26 et al., 2017; Kohout et al., 2014, 2016; Shackleton, 1982). It is relevant to ask if the freeze bonds within a broken and
27 refrozen ice cover form the weakest link at which wave-induced cracks initiate and propagate. During the wave-ice
28 interaction, the freeze bonds deform and failure occurs under a tensile state of stress arising from flexural deformation.
29 To our knowledge, no data on freeze-bond strength under tensile loading have been published.

30

31 The strength of freeze bonds has been tested only under combined compressive and shear loading. Such tests
32 have been related to continuum modeling of ice rubble using material models having yield surfaces resembling that



33 of a Mohr-Coulomb material model (Ettema and Urroz, 1989; Heinonen, 2004; Liferov et al., 2002, 2003; Serré,
34 2011b, 2011a). The critical shear stress of a Mohr-Coulomb material is given by $\tau = c + \sigma \tan \varphi$, where c is the
35 cohesion, σ the compressive stress, and φ the internal friction angle of the material. The underlying assumption in
36 testing has been that the failure of the individual freeze bonds within the rubble occurs through the same mode as the
37 failure of the rubble itself. No evidence of this type of similarity between the two scales exists. Instead, the numerical
38 simulations (Polojärvi and Tuhkuri, 2013) suggest that the individual freeze bonds within deforming rubble do not
39 fail due to shear, but rather under tensile stresses as the bonded ice blocks move relative to each other. This implies
40 that data on the shear strength of the freeze bonds may not lead to reliable estimates of the shear strength of ice rubble.
41

42 In this paper, the strength of freeze bonds under tensile loading is studied. For this purpose, we conducted
43 four-point-bending tests using the apparatus described and used by Murzda et al. (2020). All procedures for testing
44 were designed with the aim of reducing the number of variables for reliable analysis: bonds were formed between
45 milled surfaces of freshwater ice specimens (termed the parent material) and bond freezing and testing were performed
46 in air under a small compressive stress of about 4 kPa. The experimental variables were the freezing time (0.5 h...100
47 h), the sample temperature (-3°C...-25°C), and the salinity of the water used to form the bond (0...35 ppt). Bond
48 strength initially increases with freezing time, but then appears to level off and to reach a plateau (i.e., to saturate)
49 over several hours. Depending on the salinity of the water from which the bond is formed, the saturation time for bond
50 strength ranges from 0.5 h to 12 h. The “saturated strength” of freshwater bonds with finer microstructure appears to
51 reach levels higher than the strength of the parent material with a larger grain size. The results from these experiments,
52 presented below, represent the first set of results on the failure of freeze bonds under tension.

53 2. Experimental procedure

54 Freshwater ice, used here as the parent material for the freeze-bonded samples, was produced in the
55 laboratory as described in Smith and Schulson (1993) and Golding and others (2010). Tap-water was frozen
56 unidirectionally from top to bottom in a cylindrical 800 L polycarbonate tank, forming pucks of ~1 m in diameter.
57 The ice was generally bubble-free and columnar-grained. Thin-section analysis showed that the average column
58 diameter, as measured in the horizontal plane normal to the direction of ice growth using the linear intercept method,
59 was 5.5 ± 1.3 mm. The c -axes were randomly oriented within, and confined to, the horizontal plane, suggesting that the
60 ice had an S2 growth texture (in the terminology of Michel and Ramseier, 1971). The ice density was 914.1 ± 1.6 kg·m⁻³
61 (Golding and others, 2010); Young’s modulus in the horizontal plane was 9.52 GPa (Snyder and others, 2016). Once
62 grown, the ice was cut into blocks and stored in plastic cooler boxes in a cold room at -10° C. Specimen preparation
63 is described in detail elsewhere (Iliescu et al., 2017; Murdza et al., 2018, 2019, 2020, n.d.).
64

65 Samples to be freeze-bonded were prepared from the ice blocks by milling them into thin plates. The plates
66 had dimensions of $h \sim 15$ mm in thickness (parallel to the long axis of the grains), $b \sim 85$ mm in width, and $l \sim 300$ mm
67 in length. Specimens were allowed to equilibrate to the test temperature for at least 24 hours prior to testing.



68

69 The plates were then cut perpendicular to their long axis into two parts. In most samples the sawn surfaces
70 were milled after cutting (more below). To initiate freeze-bond growth, the sawn and milled surfaces were sprayed
71 with a fine mist of water at a temperature of +2°C and quickly brought into contact by setting the two pieces into a
72 freeze-bonding rig (Figure 1) in a cold room. The surfaces were wet when brought into contact, but in addition, a
73 syringe was used to inject about 0.1 ml of water to the bond to ensure uniform wetting of the surfaces. Excess water,
74 if any was observed around the bond, was wiped with a tissue. All of the above steps were performed at +2 °C to
75 prevent freezing from occurring before setting the sample into the rig.

76

77 To investigate whether the roughness of the faces in contact affects the bond strength, a few samples had
78 their faces produced by cutting the parent plate either with a coarse (1/2 inch in width, 1/40 inch in thickness and
79 6 teeth per inch) or a fine (13/64 inch in width, 1/64 inch in thickness and 24 teeth per inch) band saw. Although few
80 in number, results from these initial experiments suggested that surface roughness of the kind we explored had no
81 significant effect on flexural strength. Thus, for all further tests (that led to the results reported below) sawn surfaces
82 were milled for consistency and reproducibility (more in Discussion).

83

84 Figure 1 shows a sketch (a) and photograph (b) of the freeze-bonding rig. The rig had a system consisting of
85 two plastic bars and two springs for applying a desired pressure (i.e., compressive stress) to the bond during freezing.
86 In the present experiments, a confining pressure of ~4 kPa was chosen which is in accordance with the maximum
87 hydrostatic pressure within submerged 10-meter-thick ice rubble mass (Ettema and Schaefer, 1986). The rig was kept
88 in a cold room of the desired temperature (i.e. from -25°C to -3°C) during freezing. The base of the rig was made from
89 an acrylic plate having low heat conductivity, ensuring the heat flux in the bond area was mainly along the long axis
90 of the sample. Wax paper was placed between the ice and the acrylic to prevent freezing of ice onto the rig. All
91 materials of the rig were such that the frictional resistance between them and ice was low. This enabled good control
92 of the confining pressure and sample alignment.

93

94 To investigate the effect of the salinity on the bond strength, fresh water and saline water of salinity ranging
95 from 2 to 35 ppt (parts per thousand), was used in spraying. Saline water was prepared in the manner described by
96 Golding et al. (2010, 2014) by adding the commercially available salt mixture “Instant Ocean” to tap water. Salinity
97 was measured using a calibrated YSI Pro30 conductivity salinity meter.

98

99 After a desired time of freezing, varying from 0.5 to ~100 h, the freeze-bonded sample was removed from
100 the rig and its flexural strength under four-point bending was measured. For this purpose, a servo-hydraulic loading
101 system (MTS model 810.14) with a custom-built four-point loading frame was utilized. The sketch of the apparatus
102 is shown in Figure 2 of Murdza et al. (2020), the photograph of the apparatus is shown in Figure 5a and the apparatus
103 is described in detail elsewhere (Iliescu et al., 2017; Murdza et al., 2018, 2019, 2020). The outer loading rollers are
104 immobile during testing while the inner loading rollers are attached to the actuator. The hydraulic actuator was driven



105 under displacement control and loading was controlled using a FlexTest-40 controller. A calibrated load cell was used
106 to measure the load.

107

108 The experiments were performed at an outer-fiber center-point displacement rate of 0.1 mm s^{-1} (or outer-
109 fiber strain rate of about $1.4 \times 10^{-4} \text{ s}^{-1}$). This displacement rate resulted in an outer-fiber stress rate of about 1 MPa s^{-1} .
110 As was indicated earlier (Murdza and others, 2020), the 0.1 mm s^{-1} displacement rate in cycling results in a period
111 of $\sim 20 \text{ s}$ which is approximately the frequency of ocean swells (Collins and others, 2015). The major outer-fiber stress
112 σ_f was calculated as:

$$\sigma_f = \frac{3PL}{4bh^2}, \quad (1)$$

113 where P is the applied load and L is the distance between the outer pair of loading cylinders and is set by the geometry
114 of the apparatus to be $L = 254 \text{ mm}$. It is important to note that in all experiments described in this paper the bond
115 formation and breaking of bonded ice occurred at the same temperature. Owing to the confining impact of the loading
116 cylinders of the 4-point flexing apparatus (see Figure 5a and Figure 2 of Murdza et al. (2020)) and to the Poisson
117 effect, a biaxial state of tension developed in the ice. Based on isotropic elasticity and plasticity theories, the minor
118 stress was approximately between one-third to one-half of the major stress.

119 3. Results and Observations

120 3.1. Flexural strength of parent material

121 Two measurements on the flexural strength of pristine ice plates, that is, plate-like samples of parent material
122 without a freeze bond, were conducted at $-10 \text{ }^\circ\text{C}$. The strength values obtained were 1.51 and 1.63 MPa . Only two
123 experiments were performed as these values compare favorably with the earlier measurements by Murdza et al. (2020)
124 on the same kind of ice using the same loading system. Murdza et al. (2020) reported that the average and the standard
125 deviation of the flexural strength at -3 , -10 and $-25 \text{ }^\circ\text{C}$ were 1.42 ± 0.16 , 1.67 ± 0.22 and $1.89 \pm 0.01 \text{ MPa}$, respectively.
126 Further, the measured values are in agreement with the data that are reviewed in Timco and O'Brien (1994), where
127 the average and standard deviation of $1.73 \pm 0.25 \text{ MPa}$ is reported for the flexural strength of freshwater ice at
128 temperatures below $-4.5 \text{ }^\circ\text{C}$.

129 3.2. Flexural strength of bonded ice

130 3.2.1. Freshwater bond

131 The experiments with a freshwater bond were conducted at -3 and $-10 \text{ }^\circ\text{C}$. The results are listed in Table 1.
132 The time for the bond formation (0.5 hours was the shortest freezing period used here, implying that the bond formed
133 in less time) is reasonably consistent with analytical estimates, Appendix A. Surprisingly, in all of these experiments,
134 the failure occurred outside of the bond. This suggests that even after only a relatively short period of freezing, the
135 strength of the freshwater bond reaches and exceeds that of the parent material. Even though the results listed in Table



136 1 show scatter, at -10°C comparison of the measured flexural strengths to those described in Section 3.1 showed that
137 they are not statistically different from the flexural strength of pristine freshwater ice samples (p -value = 0.21 and 0.08
138 for tests at -3 and -10°C , respectively). This is important because it indicates that the above-described bond generation
139 procedure did not hamper the samples by, for example, leading to geometrical misalignments in them.

140 3.2.2. Saline bond

141 Figures 2 and 3 show the results from the experiments performed to investigate the effect on bond strength
142 of the salinity of the water used to create the freeze bond. The data are given in Tables 2-4. The tables indicate the
143 experiments where no freezing occurred (“No”) and the experiments where bonding occurred, but the bond was too
144 weak to be tested (“Low”). These data are excluded in the figures below.

145
146 Figure 2 shows that the strength of the saline bonds increases over time and levels off, or saturates, after
147 about 6-12 h. Thus, the strength of the saline bonds increases at a considerably lower rate than that of the freshwater
148 bonds. The reason is likely related to the rejected salts and entrapped air at the ice-water interface that slows the rate
149 of the interface advance. A comparison of these results to those in Section 3.1 shows that the strength of the saline
150 bonds is well below the strength of the freshwater ice used as the parent material. A comparison of the two data sets
151 in Figure 2 shows that the saturated strength of the bonds made from water of higher salinity but at lower temperature
152 (35 ppt and -10°C) is about twice of that of the bonds with lower salinity but higher temperature (12 ppt and -3°C).

153 Figure 3 illustrates how the salinity of the water used to generate the freeze-bond at -3°C affects its saturated
154 strength at -3°C . While the measured strength values for low salinities are close to those measured for freshwater ice,
155 the bond strength decreases rapidly with an increase in salinity and no freezing occurs once the salinity of the salt
156 water used to generate the bond reaches ~ 25 ppt; even at 17 ppt some bonds were too weak to be tested. This agrees
157 reasonably well with analytical estimates, Appendix B, where formulas that relate strength to volume fraction of solid
158 phase suggest that at salinities of 30 ppt and above at -3°C no freezing occurs. Figure 3 additionally shows two
159 exponential fits, one directly fitted to our data and one by Timco and O’Brien (1994) for the flexural strength of saline
160 ice (equations for these fits provided in Appendix C, where σ_b is flexural strength in MPa and v_b is liquid brine content
161 in parts per thousand). It is important to notice that the fit by Timco and O’Brien (1994) yields lower values than the
162 measured bond strength in the present study for the whole range of salinities used. Likewise, the actual strength values
163 for the freshwater bonds are greater than the ones suggested by Figure 3, since the failure in these cases occurred
164 outside the bond, indicating that the bond is stronger than the parent material. Both saline and freshwater bonds that
165 develop through freezing appear to reach strengths higher than that of S2 type parent material of the same salinity
166 (strength of saline parent material is assumed to be the same as in Timco and O’Brien (1994)).

167 Temperature has a strong effect on the saturated strength of the freeze bonds. Figure 4 and Table 5 summarize
168 the data from experiments on specimens having bonds made from water of salinity 20 ppt at temperatures from -3°C
169 to -25°C . Three out of the four specimens at -25°C failed outside of the bond with a measured strength of
170 1.61 ± 0.12 MPa, which is close to 1.89 MPa measured earlier at -25°C on the same type of freshwater ice (Murda
171 and others, 2020). Figure 4 also suggests that no freezing occurs at temperatures above about -3°C , which is in fair



172 agreement with analytical estimates of no strength at $T = -2\text{ °C}$ in Appendix B. Though the analytical equation from
173 Appendix B predicts well when no freezing occurs, it does not yield a trend that describes most of the data in Figure
174 4. The reason may be that for the microstructure of bonds in the present study, strength may not be directly proportional
175 to volume fraction of the solid phase as the model in Appendix B assumes, but rather a non-linear function of the
176 volume fraction of solid.

177 Figure 5a-c show an example of the typical samples after failure. Figure 5a shows a case where the crack had
178 initiated at the bond and started to propagate along it, but then deviated from it and continued to grow through the
179 parent material. Figure 5b shows a close up of a bond face-on after the most common type of failure, which occurred
180 along the bond. In this case, both surfaces of the failed freeze-bond had a fairly uniform “blurry” appearance which
181 indicates that failure occurred through the ice of the bond. It was also fairly usual for the samples having low salinities,
182 low temperatures and long freezing times, that the crack initiated and started to propagate along the bond and then
183 slightly deviated and moved parallel to the bond but inside the parent material, as shown by Figure 5c.

184 4. Discussion

185 The above results are the first measurements to be reported for the strength of freeze bonds under tensile
186 loading. Although the experiments were performed under flexural loading, they provide unique data on the tensile
187 strength of the freeze bonds. Under the loading conditions, the flexural strength of ice is governed by tensile strength,
188 although measured strengths are greater by a factor of about 1.7 than strengths measured under pure tensile loading
189 (Ashby and Jones, 2013). Murdza and others (2020) showed that the flexural strength of freshwater S2 ice tested on
190 the same loading system as used here compares well with direct measurements of the tensile strength of the same type
191 of ice at the same conditions (Carter, 1971) when divided by 1.7. By using this factor to scale the values for saturated
192 bond strengths shown in Figure 2 leads to tensile strength values of about 0.3 MPa and 0.18 MPa for bonds at -10 °C
193 and -3 °C , respectively.

194
195 While there are no other data on the tensile strength of freeze bonds, the results can be compared to the
196 relatively large amount of earlier work on the shear strength of freeze bonds (Bailey et al., 2012; Boroojerdi et al.,
197 2020a, 2020b; Bueide and Høyland, 2015; Ettema and Schaefer, 1986; Helgøy et al., 2013a, 2013b; Marchenko and
198 Chenot, 2009; Repetto-Llamazares et al., 2011b, 2011a; Shafrova and Høyland, 2008). Common values for the shear
199 strength in those studies ranged from 0.01 to 0.1 MPa, which are considerably lower than the flexural strength values
200 measured here. Usually, these strengths have been measured for bonds grown under water over periods that have not
201 been long enough to reach saturated bond strengths. On the other hand, the highest reported shear strength values
202 $\sim 0.3 \dots 0.7\text{ MPa}$ (Bailey et al., 2012; Boroojerdi et al., 2020b; Shafrova and Høyland, 2008) are within the same range
203 as the flexural strength values measured here. Given that the tensile strength of ice is, on average, lower than the shear
204 strength (Timco and Weeks, 2010), the strength values measured here are perhaps surprisingly high. The high strength
205 values here likely relate to the well-controlled bond growing procedure and possibly to a finer microstructure of the
206 material that comprises the bond.



207

208 Work on the shear strength of freeze bonds has led to a conclusion that the evolution of the bond strength has
209 three phases (Boroogerdi et al., 2020b; Repetto-Llamazares et al., 2011b, 2011a): (1) an initial period of a few minutes
210 of increasing strength due to heat flux from the bond to the parent material, (2) a period of some hours of weakening
211 as the temperature of the bond increases due to water surrounding it and (3) a period of several days of strengthening
212 due to sintering. The evolution of the flexural strength of the bonds in the present experiments is likely similar to that
213 of phases (1) and (3). The initial bond strengthening can be related to the transfer of heat along the long axis of the
214 specimen and the accompanying advance of the ice/water interface. Given that the water layer after wetting the contact
215 surfaces is very thin, the bond strength would be expected to saturate quickly; Appendix A describes a simple model
216 and suggests that the process, similar to above described phase (1), takes fewer than 10 minutes at -10 °C and a greater
217 amount of time of about 1.5 h at -3 °C, aligning with earlier studies and the result here. This means that for saline
218 bonds, phase (3) has a duration of about 6...12 hours, whereas earlier experiments have occasionally had relatively
219 long freezing times, varying from 60 h to 12 days (Bailey et al., 2012; Shafrova and Høyland, 2008).

220

221 As part of the studies on the evolution of bond strength, it has been fairly common to investigate the ratio of
222 the bond strength values to that of the parent material (Bailey et al., 2012; Boroogerdi et al., 2020b; Shafrova and
223 Høyland, 2008). Shafrova and Høyland (2008) found that specimens with bonds grown in the field had the strength
224 ratio varying from 0.008 to 0.082 (with a mean of 0.03 after 48 hours of bonding). For laboratory-grown bonds, they
225 measured ratios in the range 0.06 to 0.69 (0.21 ± 0.12). The latter values are in line with values reported by Bailey et
226 al. (2011) and Boroogerdi et al. (2020b), who reported ratios up to about 0.70 and 0.85, respectively. Boroogerdi et al.
227 (2020b) suggested an empirical formula to describe the strengthening of a freeze bond during the above-described
228 phase (3). The formula was based on curve fitting and an assumption that the shear strength of the bond approaches
229 asymptotically that of the parent material with increasing sintering time. The experiments here indicate that such an
230 assumption may not be always justified, as at least the flexural strength of the freeze bonds can reach values that are
231 above that of the parent material.

232

233 Ettema and Schaefer (1986) and Repetto-Llamazares et al. (2011b) studied whether freezing in the presence
234 of water has an effect on the shear strength of the freeze-bond. The results indicate that shear strength was higher
235 when bonds froze under water. While Ettema and Schaefer (1986) let the bonding occur with samples submerged in
236 fresh water, Repetto-Llamazares et al. (2011b) used 7 ppt saline water for submerging. Earlier studies on the effect of
237 freezing conditions have not had the opposing surfaces wetted before bringing them together when generating bonds
238 in air. This effectively removes the above-described phase (1) from the bond strength evolution, if the result of the
239 heat transfer during the initial period of bond strengthening is assumed to simply be freezing of the liquid at the bond
240 interface. In addition, in these earlier studies, the maximum freezing times for the bonds grown in air varied only
241 from 0.5 min to 3 min. As phase (3) takes at least several hours, it seems likely that the mentioned studies have not
242 yielded data on saturated bond strengths for bonds grown in air.

243



244 While the new data from the present tests yielded clear trends for the strength of the freeze-bonds, they also
245 showed significant scatter. This scatter, even when bond generation was performed in a simplified manner using
246 carefully prepared milled samples (Section 2), is an indication that the strength of freeze bonds is a parameter that
247 inherently shows wide scatter. One reason for this, amongst others perhaps, is the detailed microstructure/phase
248 distribution of the bond. The microstructure probably varies somewhat from specimen to specimen, thereby leading
249 to variations in bond strength. The variation is actually of similar magnitude to that observed in experiments on the
250 flexural strength of pristine ice samples made with the same apparatus (Murdza et al., 2020).

251

252 The fact that in samples with freshwater bonds failure initiated and propagated outside of the bond suggests
253 that the strength of the freshwater bond is greater than the strength of pristine freshwater S2 ice. This may indicate a
254 difference in microstructure between the ice in the freeze bond and the ice of the parent plates. A finer grain size
255 within the bonds may be due to the initial water layer, which was produced by spraying a very fine mist, creating small
256 water droplets working as nucleation sites for the ice grains in the bond. Our argument is supported by the work of
257 Schulson and others (1984) who showed that tensile strength strongly depends on the grain size, increasing as grain
258 size decreases. A difference in grain size could also explain the fact that the strength versus salinity curve from Timco
259 and O'Brien (1994) is below the trend obtained in the present study (Figure 3). Concerning of the microstructure of
260 the bonds, one may think that because one phase is dominant it should form the matrix; however, there is at least one
261 class of materials, namely high-temperature nickel-based superalloys (Sims, 1984) where the minor component forms
262 the matrix. Since we do not know the structure of the bonds in the present study, we cannot be conclusive in this
263 regard.

264

265 As one may have expected, both temperature and salinity affect the flexural strength of bonded ice samples.
266 The trend of strength versus salinity (Figure 3) has an exponential functionality similar to what has been suggested by
267 Timco and O'Brien (1994), while the trend of strength versus temperature (Figure 4) appears, to a first approximation,
268 to be roughly linear. It is important to mention here that the salinities provided in this paper are salinities of the spray
269 and not of melt-water from the bond itself, and this begs the question: Is the bond salinity the same or lower than the
270 salinity of spray solution? In the formation of a natural floating sea ice cover, of course, the rejection of salts from
271 ice results in melt-water salinities lower than bulk water salinity. (Weeks and Ackley, 1986) . Given that in our
272 experiments the bond thickness is very small (<1 mm) and freezing time is relatively short, it is unlikely that all the
273 salt is expelled from the freeze bond, resulting in the bond salinity similar to the spray salinity. Therefore, while the
274 resulting bonds might have salinities slightly lower than the sprayed water, the results yield a reasonably reliable trend
275 of strength as a function of salinity which is very similar to the relationship proposed by Timco and O'Brien (1994).

276

277 The effect of surface roughness at the freezing interface was also briefly addressed when performing the
278 experiments. In addition to the milled surfaces with a roughness of $0.43 \pm 0.24 \times 10^{-6}$ m in the direction of milling and
279 $2.01 \pm 0.47 \times 10^{-6}$ m in the orthogonal direction (Schulson and Fortt, 2012), experiments were performed on samples
280 with surfaces produced by using a fine and coarse band saw blade, which resulted in ice surface roughness of up to



281 ~1 mm. The results from the experiments with differently produced surfaces showed no significant difference on the
282 strength of freshwater and saline bonds (1.39 MPa vs 1.43±0.15 MPa for freshwater bonds and 0.39±0.13 MPa vs
283 0.34±0.16 MPa for saline bonds of 12 ppt salinity). As milling could be performed with the highest accuracy from the
284 aspect of sample dimensions and alignment, it was chosen as the technique we used here. Unlike what was observed
285 in the present study, Helgøy et al. (2013a) observed that the surface roughness does affect freeze bond shear strengths,
286 with rougher surface leading to bonds having higher strength. The discrepancy between their results and results in the
287 present study suggests that there may exist a threshold value for the surface roughness, after which it affects the bond
288 strength; it is likely that both milled and sawn surfaces used in the present study are too smooth for the effect of surface
289 roughness to be observed. On the other hand, experiments on shear strength usually involve sliding motion between
290 the blocks of the parent material. This motion may become restricted by rough surfaces, which could lead to higher
291 shear loads interpreted to be due to an increase in freeze-bond strength. In tests under tensile loading, such kinematic
292 restrictions do not exist.

293

294 Finally, it is worth noting that while this is the first study on the flexural strength of freeze bonds, it is not
295 the complete story. Further work is needed to investigate the effects of other factors such as bond pressure, the
296 character of parent ice plate, bond microstructure, the width of the opening to be bonded, etc.

297 5. Conclusions

298 Systematic experiments on the flexural strength of freeze bonds were conducted for the first time. The bonds
299 were grown in the air under 4 kPa confining pressure. The parent material was S2 columnar-grained freshwater ice.
300 The salinity of the bond varied from 0 to 35 ppt and freezing temperatures from -3 to -25 °C. It is concluded that:

- 301 (i) Freshwater bond strength exceeds the strength of parent ice in less than 0.5 h upon freezing.
- 302 (ii) The saline bonds reach their saturated strength within about 6-12 h of freezing.
- 303 (iii) An increase in bond salinity and in freezing temperature leads to a decrease in bond strength.
- 304 (iv) The relationship between bond strength and its salinity is similar to the one suggested by Timco and O'Brien
305 (1994).
- 306 (v) No freezing occurs once the salinity of the water used to generate the bond reaches values of about ~25 ppt
307 at -3 °C.

308 Acknowledgements

309 The authors are grateful for the financial support from the Academy of Finland through the project no. 309830 (“Ice
310 Block Breakage: Experiments and Simulations (ICEBES)”) and National Science Foundation (FAIN 1947-107). Arttu
311 Polojärvi worked on the article while visiting Thayer School of Engineering at Dartmouth College (Hanover, NH,



312 USA) during spring 2020, thanks are extended to Prof. Erland Schulson for hosting. Finnish Maritime Foundation is
313 acknowledged for partial funding of the visit.

314

315 **Author contributions:** AM, AP, ES, and CR designed the experiments, and AM carried them out. AM and AP
316 prepared the manuscript with contributions from all co-authors.

317

318 **Competing interests:** The authors declare that they have no conflict of interest.

319 References

320 Ardhuin, F., Otero, M., Merrifield, S., Grouazel, A. and Terrill, E.: Ice Breakup Controls Dissipation of Wind Waves
321 Across Southern Ocean Sea Ice, *Geophys. Res. Lett.*, 47(13), doi:10.1029/2020GL087699, 2020.

322 Ashby, M. F. and Jones, D. R. H.: *Engineering materials 2: an introduction to microstructures and processing*,
323 Elsevier/Butterworth-Heinemann, Oxford., 2013.

324 Asplin, M. G., Galley, R., Barber, D. G. and Prinsenber, S.: Fracture of summer perennial sea ice by ocean swell as
325 a result of Arctic storms, *J. Geophys. Res. Ocean.*, 117(6), 1–12, doi:10.1029/2011JC007221, 2012.

326 Bailey, E., Sammonds, P. R. and Feltham, D. L.: The consolidation and bond strength of rafted sea ice, *Cold Reg. Sci.*
327 *Technol.*, 83–84, 37–48, doi:10.1016/j.coldregions.2012.06.002, 2012.

328 Boroojerdi, M. T., Bailey, E. and Taylor, R.: Experimental investigation of rate dependency of freeze bond strength,
329 *Cold Reg. Sci. Technol.*, 178, 1–12, doi:10.1016/j.coldregions.2020.103120, 2020a.

330 Boroojerdi, M. T., Bailey, E. and Taylor, R.: Experimental study of the effect of submersion time on the strength
331 development of freeze bonds, *Cold Reg. Sci. Technol.*, 172, 1–16, doi:10.1016/j.coldregions.2019.102986, 2020b.

332 Bueide, I. M. and Høyland, K. V.: Confined compression tests on saline and fresh freeze-bonds, in *Proceedings of the*
333 *23rd International Conference on Port and Ocean Engineering under Arctic Conditions*, Trondheim, Norway., 2015.

334 Carter, D.: *Lois et mechanisms de l'apparente fracture fragile de la glace de riviere et de lac*, PhD Thesis, University
335 of Laval., 1971.

336 Collins, C. O., Rogers, W. E., Marchenko, A. and Babanin, A. V.: In situ measurements of an energetic wave event
337 in the Arctic marginal ice zone, *Geophys. Res. Lett.*, 42(6), 1863–1870, doi:10.1002/2015GL063063, 2015.

338 Ettema, R. and Schaefer, J. A.: Experiments on Freeze-Bonding Between Ice Blocks in Floating Ice rubble, *J. Glaciol.*,
339 32(112), 397–403, doi:10.3189/S0022143000012107, 1986.

340 Ettema, R. and Urroz, G. E.: On internal friction and cohesion in unconsolidated ice rubble, *Cold Reg. Sci. Technol.*,
341 16(3), 237–247, doi:10.1016/0165-232X(89)90025-6, 1989.

342 Frankenstein, G. and Garner, R.: Equations for Determining the Brine Volume of Sea Ice from -0.5° to -22.9°C ., *J.*
343 *Glaciol.*, 6(48), 943–944, doi:10.3189/S0022143000020244, 1967.

344 Golding, N., Schulson, E. M. and Renshaw, C. E.: Shear faulting and localized heating in ice: The influence of
345 confinement, *Acta Mater.*, 58, 5043–5056, doi:10.1016/j.actamat.2010.05.040, 2010.

346 Golding, N., Snyder, S. A., Schulson, E. M. and Renshaw, C. E.: Plastic faulting in saltwater ice, *J. Glaciol.*, 60(221),



- 347 447–452, doi:10.3189/2014JoG13J178, 2014.
- 348 Heinonen, J.: Constitutive modeling of ice rubble in first-year ridge keel, Aalto University., 2004.
- 349 Helgøy, H., Astrup, O. S. and Høyland, K. V.: Laboratory work on freeze-bonds in ice rubble, Part I: Experimental
350 set-up, Ice-properties and freeze-bond texture, in Proceedings of the 22nd International Conference on Port and Ocean
351 Engineering under Arctic Conditions, Espoo, Finland., 2013a.
- 352 Helgøy, H., Astrup, O. S. and Høyland, K. V.: Laboratory work on freeze-bonds in ice rubble, Part II – Results from
353 individual freeze bond experiments, in Proceedings of the 22nd International Conference on Port and Ocean
354 Engineering under Arctic Conditions, Espoo, Finland., 2013b.
- 355 Hwang, B., Wilkinson, J., Maksym, E., Graber, H. C., Schweiger, A., Horvat, C., Perovich, D. K., Arntsen, A. E.,
356 Stanton, T. P., Ren, J. and Wadhams, P.: Winter-to-summer transition of Arctic sea ice breakup and floe size
357 distribution in the Beaufort Sea, *Elem Sci Anth*, 5, 40, doi:10.1525/elementa.232, 2017.
- 358 Iliescu, D., Murdza, A., Schulson, E. M. and Renshaw, C. E.: Strengthening ice through cyclic loading, *J. Glaciol.*,
359 63(240), 663–669, doi:10.1017/jog.2017.32, 2017.
- 360 Kohout, A. L., Williams, M. J. M., Dean, S. M. and Meylan, M. H.: Storm-induced sea-ice breakup and the
361 implications for ice extent, *Nature*, 509(7502), 604–607, doi:10.1038/nature13262, 2014.
- 362 Kohout, A. L., Williams, M. J. M., Toyota, T., Lieser, J. and Hutchings, J.: In situ observations of wave-induced sea
363 ice breakup, *Deep. Res. Part II Top. Stud. Oceanogr.*, 131, 22–27, doi:10.1016/j.dsr2.2015.06.010, 2016.
- 364 Liferov, P., Jensen, A. and Høyland, K. V.: On analysis of punch tests on ice rubble, in Proceedings of the 16th
365 International Symposium on Ice, volume 2, pp. 101–110, Dunedin, New Zealand., 2002.
- 366 Liferov, P., Jensen, A. and Høyland, K. V.: 3D finite element analysis of laboratory punch tests on ice rubble, in
367 Proceedings of the 17th International Conference on Port and Ocean Engineering under Arctic Conditions, POAC'03,
368 volume 2, pp. 611–621, Trondheim, Norway., 2003.
- 369 Marchenko, A. and Chenot, C.: Regelation of ice blocks in the water and on the air, in Proceedings of the 20th
370 International Conference on Port and Ocean Engineering under Arctic Conditions, Luleå, Sweden., 2009.
- 371 Michel, B. and Ramseier, R. O.: Classification of river and lake ice, *Can. Geotech. J.*, 8(1), 36–45, doi:10.1139/t71-
372 004, 1971.
- 373 Murdza, A., Schulson, E. M. and Renshaw, C. E.: Hysteretic behavior of freshwater ice under cyclic loading :
374 preliminary results, in 24th IAHR International Symposium on Ice, pp. 185–192, Vladivostok., 2018.
- 375 Murdza, A., Schulson, E. M. and Renshaw, C. E.: The Effect of Cyclic Loading on the Flexural Strength of Columnar
376 Freshwater Ice, in Proceedings of the 25th International Conference on Port and Ocean Engineering under Arctic
377 Conditions, Delft, Netherlands., 2019.
- 378 Murdza, A., Schulson, E. M. and Renshaw, C. E.: Strengthening of columnar-grained freshwater ice through cyclic
379 flexural loading, *J. Glaciol.*, 66(258), 556–566, doi:10.1017/jog.2020.31, 2020.
- 380 Murdza, A., Schulson, E. M. and Renshaw, C. E.: Behavior of Saline Ice under Cyclic Flexural Loading, *Cryosph.*,
381 Under Review, n.d.
- 382 Polojärvi, A. and Tuhkuri, J.: On modeling cohesive ridge keel punch through tests with a combined finite-discrete
383 element method, *Cold Reg. Sci. Technol.*, 85, 191–205, doi:10.1016/j.coldregions.2012.09.013, 2013.



- 384 Repetto-Llamazares, A. H. V., Høyland, K. V. and Kim, E.: Experimental studies on shear failure of freeze-bonds in
385 saline ice: Part II: Ice-ice friction after failure and failure energy, *Cold Reg. Sci. Technol.*, 65(3), 298–307,
386 doi:10.1016/j.coldregions.2010.12.002, 2011a.
- 387 Repetto-Llamazares, A. H. V., Høyland, K. V. and Evers, K. U.: Experimental studies on shear failure of freeze-bonds
388 in saline ice: Part I. Set-up, failure mode and freeze-bond strength, *Cold Reg. Sci. Technol.*, 65(3), 286–297,
389 doi:10.1016/j.coldregions.2010.12.001, 2011b.
- 390 Schulson, E. M. and Fortt, A. L.: Friction of ice on ice, *J. Geophys. Res. Solid Earth*, 117(B12), n/a-n/a,
391 doi:10.1029/2012JB009219, 2012.
- 392 Schulson, E. M., Lim, P. N. and Lee, R. W.: A brittle to ductile transition in ice under tension, *Philos. Mag. A*, 49(3),
393 353–363, doi:10.1080/01418618408233279, 1984.
- 394 Serré, N.: Mechanical properties of model ice ridge keels, *Cold Reg. Sci. Technol.*, 67(3), 89–106,
395 doi:10.1016/j.coldregions.2011.02.007, 2011a.
- 396 Serré, N.: Numerical modelling of ice ridge keel action on subsea structures, *Cold Reg. Sci. Technol.*, 67(3), 107–119,
397 doi:10.1016/j.coldregions.2011.02.011, 2011b.
- 398 Shackleton, E. H.: *South: The Story of Shackleton’s Last Expedition, 1914–17*, Macmillan, USA., 1982.
- 399 Shafrova, S. and Høyland, K. V.: The freeze-bond strength in first-year ice ridges. Small-scale field and laboratory
400 experiments, *Cold Reg. Sci. Technol.*, 54(1), 54–71, doi:10.1016/j.coldregions.2007.11.005, 2008.
- 401 Shen, H. H.: *Wave-Ice Interactions*, in *Encyclopedia of Maritime and Offshore Engineering*, John Wiley & Sons, Ltd,
402 Chichester, UK., 2017.
- 403 Sims, C. T.: A History of Superalloy Metallurgy for Superalloy Metallurgists, in *Superalloys 1984 (Fifth International
404 Symposium)*, pp. 399–419, The Minerals, Metals and Materials Society, Warrendale, PA., 1984.
- 405 Smith, T. R. and Schulson, E. M.: The brittle compressive failure of fresh-water columnar ice under biaxial loading,
406 *Acta Metall. Mater.*, 41(1), 153–163, doi:10.1016/0956-7151(93)90347-U, 1993.
- 407 Snyder, S. A., Schulson, E. M. and Renshaw, C. E.: Effects of prestrain on the ductile-to-brittle transition of ice, *Acta
408 Mater.*, 108, 110–127, doi:10.1016/j.actamat.2016.01.062, 2016.
- 409 Squire, V. A.: Ocean Wave Interactions with Sea Ice: A Reappraisal, *Annu. Rev. Fluid Mech.*, 52(1), 37–60,
410 doi:10.1146/annurev-fluid-010719-060301, 2020.
- 411 Timco, G. W. and O’Brien, S.: Flexural strength equation for sea ice, *Cold Reg. Sci. Technol.*, 22(3), 285–298,
412 doi:10.1016/0165-232X(94)90006-X, 1994.
- 413 Timco, G. W. and Weeks, W. F.: A review of the engineering properties of sea ice, *Cold Reg. Sci. Technol.*, 60(2),
414 107–129, doi:10.1016/J.COLDREGIONS.2009.10.003, 2010.
- 415 Weeks, W. F. and Ackley, S. F.: *The Growth, Structure, and Properties of Sea Ice*, in *The Geophysics of Sea Ice*, pp.
416 9–164, Springer US, Boston, MA., 1986.
- 417
- 418
- 419
- 420



421 **Appendix A: Time for the freeze-bond formation**

422 To estimate the time to form a freeze-bond we assume that heat fluxes are along the long axis of the sample,
423 i.e. horizontal temperature gradients are much larger than vertical gradients at the freezing interface. The other
424 assumptions are that the heat flow through a material is equal to the energy for the solidification of the water along
425 the bond and that no heat losses occur, i.e.

426

$$k \frac{dT}{dx} = \rho \lambda \frac{dx}{dt} \quad (\text{A1})$$

427

428 where t is the time, T is the ice temperature, k is the thermal conductivity of ice, λ is the latent heat of fusion of ice
429 per unit mass, ρ is the ice density and Δx is the characteristic conduction length or, in our case, the thickness of the
430 bond.

431 Taking into account that thermal diffusivity $\alpha = k/\rho c_p$, where c_p is specific heat capacity, and that $x = \sqrt{\alpha t}$,
432 after integration of Equation A1 we obtain the relationship:

433

$$t = \frac{1}{4} \left(\frac{x\lambda}{\Delta T} \right)^2 \left(\frac{\rho}{kc_p} \right) \quad (\text{A2})$$

434

435 A note of caution is necessary here. As ice-water interface advances during freezing in saline ice, both air
436 and salt are rejected and build up at the interface. Unlike freezing in nature, there is not enough space for rejection
437 and, as a result, this slows the rate of advance of the interface.

438

439 According to Equation A2, and using parametric values of $c_p = 2100 \text{ J/kg}^\circ\text{C}$, $\lambda = 330 \text{ kJ/kg}$, $k =$
440 $2.2 \text{ W/m}^\circ\text{C}$, $\rho = 914 \text{ kg/m}^3$ for freshwater ice at $-10 \text{ }^\circ\text{C}$ and bond thickness of 1 mm we need only 1 min for the
441 bond formation, while for freshwater ice at $-3 \text{ }^\circ\text{C}$ a similar bond forms in about 10 minutes. While this estimate is
442 consistent with observations, it is also in accord with earlier experimental results by Repetto-Llamazares et al. (2011a,
443 2011b) and Borojeerdi et al. (2020a) for phase (1) increase during freeze bond shear strength evolution (Section 4).

444

445 **Appendix B: The strength of freeze-bonds as a function of salinity and temperature**

446 Principle:

447

448 The freeze bond is comprised of essentially two phases, solid (ice) plus liquid (water), barring entrapped air.
449 To a first approximation, we assume that its strength, σ_{fb} , is proportional to the volume fraction, f_s , of the solid phase.
450 The constant of proportionality, σ_{f0} , is the strength of freshwater ice. The relationship:



$$\sigma_{fb} = \sigma_{f0} f_s. \quad (\text{A3})$$

451 The volume fraction of the solid phase is obtained from the lever rule:

$$f_s = \frac{X_l - X_0}{X_l - X_s}, \quad (\text{A4})$$

452 where X_l and X_s denote the limit of solubility of salt in the liquid (water) and in the solid (ice) phases, respectively,
453 and X_0 is the concentration of salt in the water before freezing is initiated. Over the temperature range of interest, the
454 phase diagram for the H₂O-NaCl system (i.e., thermodynamics) dictates that both X_l and X_s increases with decreasing
455 temperature, T , according to the relationships:

$$X_l = \frac{T - T_0}{m_l}, \quad (\text{A5})$$

$$X_s = \frac{T - T_0}{m_s}, \quad (\text{A6})$$

456 where T_0 denotes the melting point of "pure" ice (273 K) and m_l and m_s , respectively, denote the slope of the liquidus
457 and the solidus on the phase diagram; both slopes are negative. The solubility of salt in ice is very low and so for
458 practical purposes $X_s \sim 0$. Writing the temperature difference as $T - T_0 = \Delta T$, the volume fraction of ice within the
459 freeze bond from Eqn (A4) is given by:

$$f_s = \left(1 - \frac{m_l X_0}{\Delta T}\right). \quad (\text{A7})$$

460 Thus, upon equating X_0 to salinity, S , the strength of the freeze bond is given by:

$$\sigma_{fb} = \sigma_{f0} \left(1 - \frac{m_l S}{\Delta T}\right). \quad (\text{A8})$$

461 Taking m_l to be independent of concentration, its value is $m_l = -0.1 \text{ Kpsu}^{-1}$, giving:

$$\sigma_{fb} = \sigma_{f0} \left(1 + \frac{0.1S}{\Delta T}\right), \quad (\text{A9})$$

462 where $\Delta T < 0$.

463

464 The model thus dictates that once freezing is complete the strength of the freeze bond decreases linearly with
465 increasing salinity, reaching the limit of zero strength when $S = \Delta T / -m_l$.

466

467 Both dictates are in reasonable agreement with observation.

468

469 Appendix C: Trends in Figure 3

470

471 The red trend in Figure 3 is taken from (Timco and O'Brien, 1994) where the authors report values for
472 flexural strength of saline ice over the range of salinities used in the present study and for temperatures above -4.5°C
473 (σ_f in MPa), i.e.



474

$$\sigma_f = 1.76e^{-5.88\sqrt{v_b}}. \quad (\text{A10})$$

475

476

477 To calculate salinity S (in ppt) based on the liquid brine content v_b (brine volume fraction) in Timco and
478 O'Brien (1994) we used the following relationship suggested by (Frankenstein and Garner, 1967):

479

$$v_b = S \left(\frac{49.185}{|T|} + 0.532 \right) \quad (\text{A11})$$

480

481 where T is the ice temperature in degrees Celsius between -0.5 °C and -22.9 °C. The fit to our data in Figure 3 (black
482 curve) was made according to the least square method which resulted in the following equation (σ_f in MPa):

483

$$\sigma_f = 1.12e^{-5.88v_b} \quad (\text{A12})$$

484

485

486

487

488

489

490

491

492

493

494

495

496

497

498

499

500

501

502

503

504

505

506



507 **Table 1. Results from testing freshwater bond experiments. The time here is the bond formation time, the strength is the**
508 **flexural strength (temperature during flexural testing and bond formation was the same). The reader should notice that in**
509 **all of these experiments the failure occurred outside of the bond and within the parent material.**

Sample #	Temperature [°C]	Time [h]	Strength [MPa]
1	-10	24	1.43
2	-10	25	1.39
3	-10	24	1.28
4	-10	3	1.58
5	-3	1.5	1.02
6	-3	1.5	1.28
7	-3	0.5	1.4

510

511 **Table 2. Results from testing saline bond experiments at -10 °C and 35 ppt.**

Sample #	Time [h]	Strength [MPa]
8	1.5	0.15
9	3	0.1
10	26	0.34
11	34	0.54
12	25	0.64
13	82	0.61
14	6	0.38
15	12	0.54

512

513 **Table 3. Results from testing saline bond experiments at -3 °C and 12 ppt.**

Sample #	Time [h]	Strength [MPa]
16	1.5	Low
17	1.5	0.31
18	3	0.17
19	3	0.18
20	6	0.25
21	6	0.22
22	14	0.48
23	24	0.14
24	24	0.35
25	72	0.29
26	97	0.32



514

515

516 **Table 4. Results from testing saline bond experiments at -3 °C.**

Sample #	Salinity [ppt]	Time [h]	Strength [MPa]
27	35	1.5	No*
28	35	24	No*
29	25	24	No*
30	20	28	0.12
31	17	3	Low*
32	17	13	Low*
33	17	25	0.3
34	17	113	0.28
35	10	24	0.34
36	10	24	0.34
37	10	24	0.41
38	10	26	0.77
39	10	73	0.54
40	5	21	0.37
41	5	24	0.46
42	5	24	0.75
43	2	25	0.62
44	2	24	0.91

517 * "No" and "Low" correspond to "No freezing occurred" and "Strength was too small to be measured", respectively.

518

519 **Table 5. Results from testing of ice with bond salinity of 20 ppt after ~24 h of freezing.**

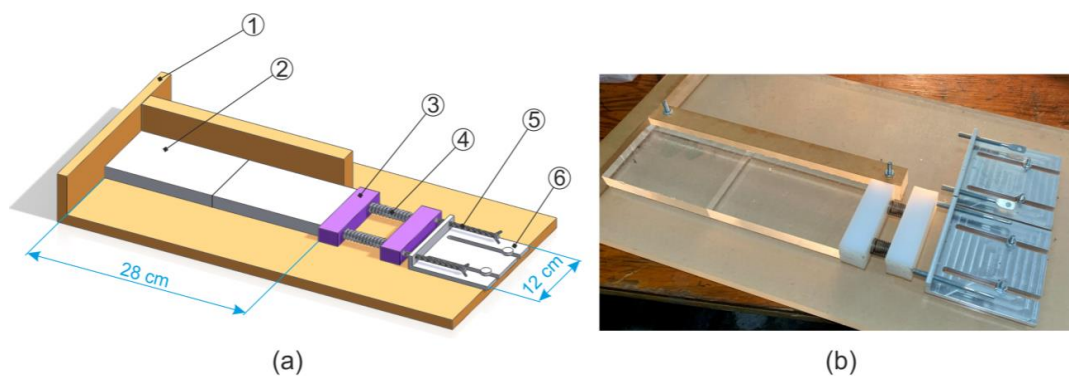
Sample #	Temperature [°C]	Strength [MPa]
45	-25	1.69*
46	-25	1.67*
47	-25	1.47*
48	-25	1.13
49	-20	1.25
50	-20	0.71
51	-15	0.87
52	-15	0.76
53	-15	0.63
54	-15	0.55
55	-15	0.35
56	-15	0.2
57	-10	0.66
58	-10	0.64



Sample #	Temperature [°C]	Strength [MPa]
59	-10	0.46
60	-10	0.4
61	-5	0.2
62	-5	0.1
63	-3	0.12

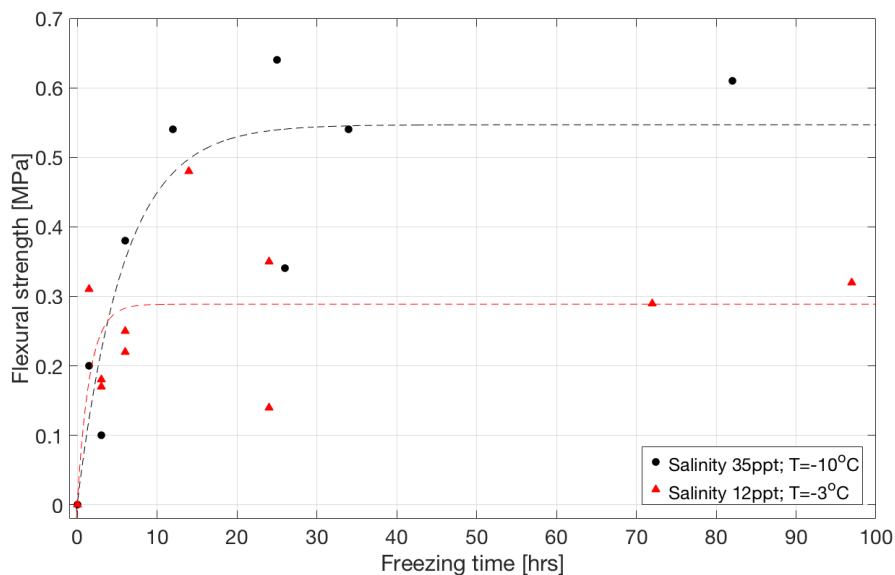
*failure occurred outside the bond.

520
521
522
523



524
525
526

Figure 1. Sketch (a) and photograph (b) of the freeze-bonding rig with an ice sample having the shape of a thin plate: 1 – acrylic plate; 2 – ice specimen; 3 – plastic bar; 4 – spring; 5 – bolt; 6 – fixation plate.

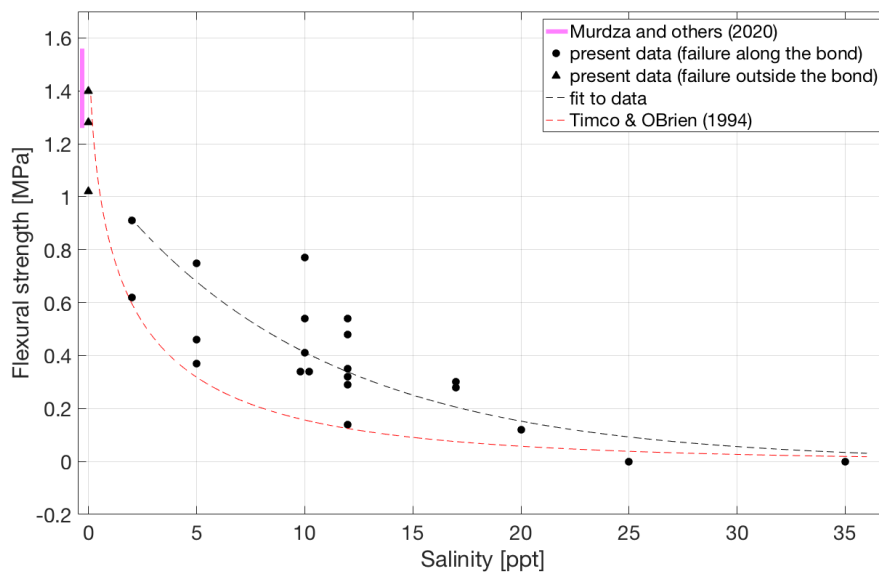


527

528

529

Figure 2. Flexural strength as a function of freezing time for bonded ice prepared from salt water of 35 ppt salinity at -10°C (in black) and from salt water of 12 ppt salinity at -3°C (in red).



530

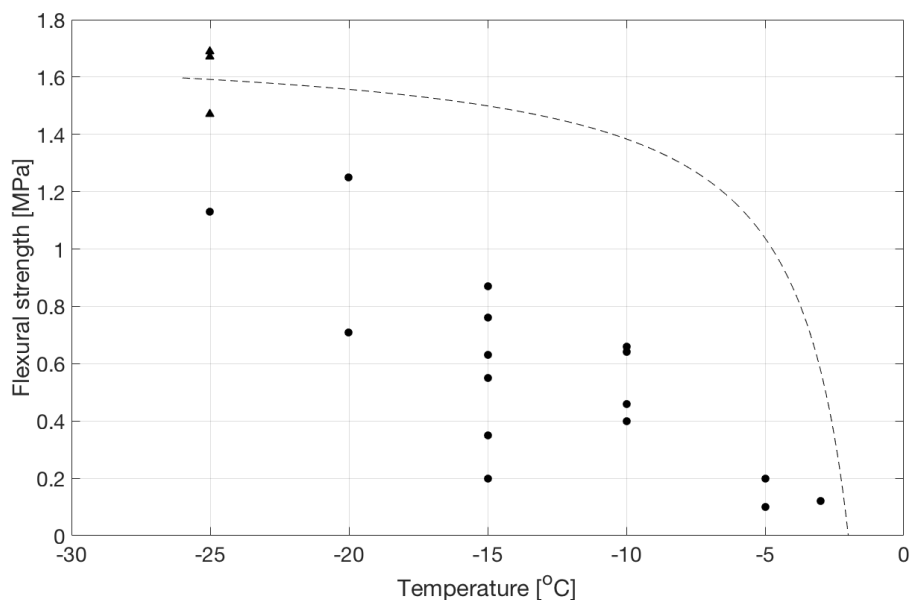
531

532

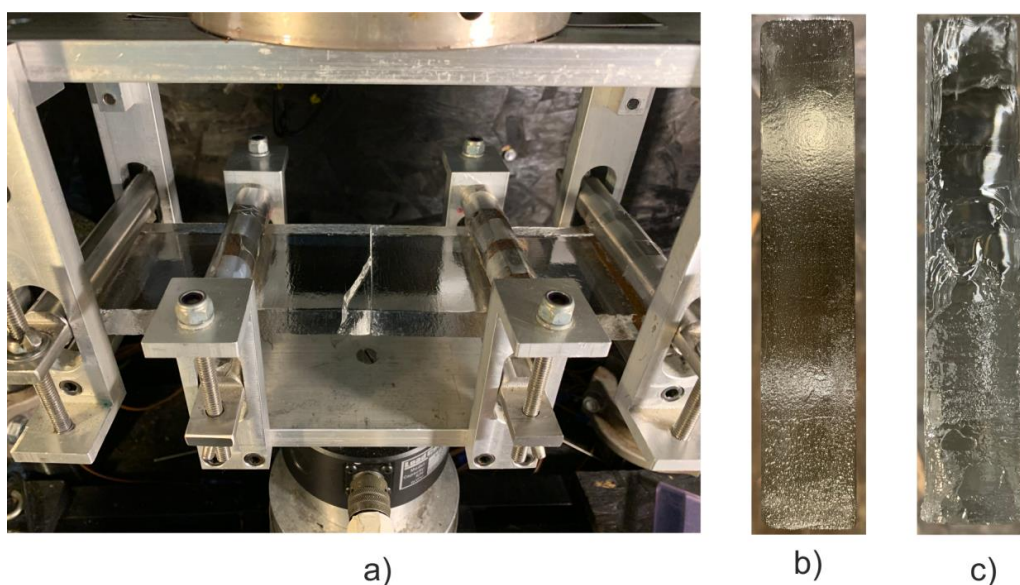
533

534

Figure 3. Flexural strength at -3 °C of bonded ice as a function of the salinity of the salt water from which the bond was formed. The solid pink line indicates the flexural strength 1.42 ± 0.16 MPa of parent freshwater ice at -3 °C (Murdza and others, 2020). A red dashed line is taken from Timco and O'Brien (1994) for the ice at -3 °C. A black dashed line is a fit to the present data.



535
536 **Figure 4.** Flexural strength of bonded ice as a function of temperature for bonds formed from water of salinity of 20 ppt.
537 **Triangular-shaped points at -25 °C indicate that actual bond strength is greater than that of the parent material as the**
538 **failure occurred outside the bond. The dotted line is drawn according to the model in Appendix B.**



539
540 **Figure 5.** Photographs of an ice sample #38 right after forced failure (a); the saline bond surface of 10 ppt after a crack
541 **propagated fully through the bond, sample #19 (b) and partially through the parent material, sample #47 (c).**

542